NUSC Technical Memorandum 841013
16 January 1984

Mean and Variance of Product Array Response: Application to a Cross-Line Array

Albert H. Nuttall
Surface Ship Sonar Department

Naval Underwater Systems Center
Newport, Rhode Island/New London, Connecticut

Report Documentation Page

Form Approved
OMB No. 0704-0188

1. REPORT DATE	2. REPORT TYPE	3. DATES COVERED
16 JAN 1984	**Technical Memo**	**16-01-1984 to 16-01-1984**

4. TITLE AND SUBTITLE
Mean and Variance of Product Array Response : Application to a Cross-Line Array

5a. CONTRACT NUMBER

5b. GRANT NUMBER

5c. PROGRAM ELEMENT NUMBER

6. AUTHOR(S)
Albert Nuttall

5d. PROJECT NUMBER
N70021 and A75205

5e. TASK NUMBER

5f. WORK UNIT NUMBER

7. PERFORMING ORGANIZATION NAME(S) AND ADDRESS(ES)
Naval Underwater Systems Center,New London,CT,06320

8. PERFORMING ORGANIZATION REPORT NUMBER
TM 841013

9. SPONSORING/MONITORING AGENCY NAME(S) AND ADDRESS(ES)
DARPA and ONR

10. SPONSOR/MONITOR'S ACRONYM(S)
DARPA; ONR

11. SPONSOR/MONITOR'S REPORT NUMBER(S)

12. DISTRIBUTION/AVAILABILITY STATEMENT
Approved for public release; distribution unlimited

13. SUPPLEMENTARY NOTES
NUWC2015

14. ABSTRACT
The mean and variance of the product of the narrowband responses of two arrays steered to the same look direction is evaluated and shown to depend on the complex coherence between the two array outputs. For a cross-line array of perpendicular equi-spaced elements, the stability is much poorer than for a sum array processor, due to the largely uncommon volume of intersection of the two cones of response of each line. When each array is extended to be planar, the degradation in stability is lessened, tending towards the sum array performance as the number of common elements increases.

15. SUBJECT TERMS
ACSAS Exploratory Development; ZR0000101; Applications of Statistical Communication Theory to Acoustic Signal Processing; Cross-Line Array

16. SECURITY CLASSIFICATION OF:			17. LIMITATION OF ABSTRACT	18. NUMBER OF PAGES	19a. NAME OF RESPONSIBLE PERSON
a. REPORT	b. ABSTRACT	c. THIS PAGE			
unclassified	**unclassified**	**unclassified**	**Same as Report (SAR)**	**31**	

TM No. 841013
Cy002

NAVAL UNDERWATER SYSTEMS CENTER
New London Laboratory
New London, Connecticut

MEAN AND VARIANCE OF PRODUCT ARRAY RESPONSE; APPLICATION TO A CROSS-LINE ARRAY

Date: 16 January 1984

Prepared by: Albert H. Nuttall

Albert H. Nuttall
Surface Ship Sonar
Department

ABSTRACT

The mean and variance of the product of the narrowband responses of two arrays steered to the same look direction is evaluated and shown to depend on the complex coherence between the two array outputs. For a cross-line array of perpendicular equi-spaced elements, the stability is much poorer than for a sum array processor, due to the largely uncommon volume of intersection of the two cones of response of each line. When each array is extended to be planar, the degradation in stability is lessened, tending towards the sum array performance as the number of common elements increases.

ADMINISTRATIVE INFORMATION

This memorandum was prepared under NUSC Project No. N70021, "ACSAS Exploratory Development", Principal Investigator Dr. C. H. Sherman, Code 3292. The sponsoring activity is DARPA and ONR, Program Manager James Webster, ONR 280. Also this memorandum was prepared under NUSC Project No. A75205, Subproject No. ZR0000101, "Applications of Statistical Communication Theory to Acoustic Signal Processing", Principal Investigator Dr. A. H. Nuttall, Code 33, Program Manager Capt. Z. L. Newcomb, Naval Material Command, MAT 05B.

The author of this technical memorandum is located at the Naval Underwater Systems Center, New London, CT 06320.

INTRODUCTION

A planar array with a grid structure of $M_1 \times M_2$ elements requires a large number of receivers and considerable signal processing when all the elements are employed and actively utilized. In an effort to conserve on the number of elements and amount of signal processing, the possibility of using a sparse array seems to have merit. In particular, it has been found that an equi-weighted planar array has the same auto spectral density response as the cross spectrum of a pair of perpendicular lines of double the length and with triangular weighting on each line. However, without investigating the variances of these sum and cross-line arrays, respectively, it is impossible to decide on their relative merits.

Here we will consider two arbitrary planar arrays (which may have some common elements and may even be linear arrays), both of which are steered to the same look direction and employ weightings for sidelobe control. The sample cross-spectral density of the two array outputs is the output variable of interest. Thus the combination of arrays is resolving in both spatial angles (wavenumber) as well as in temporal frequency. We will evaluate the mean and variance of the cross-spectral density estimate at the system output in terms of the statistical properties of the impingent noise field and the array parameters, such as look direction and weighting.

As a special case, by choosing the two planar arrays identical in element usage and weighting, we will reduce to the sum array since the cross-spectrum then becomes the auto-spectrum. Thus we can compare the performances of product arrays and sum arrays in terms of the mean and variance of their responses.

CROSS-SPECTRAL DENSITY ESTIMATE

Let $x(t)$ and $y(t)$ be any two array outputs which are stationary in time, zero-mean, and have auto-spectra and cross-spectrum $G_x(f)$, $G_y(f)$, $G_{xy}(f)$, respectively. f is temporal frequency in Hz. Sections of each waveform are gated out by multiplying by temporal weightings and then subjected to Fourier analysis according to*

$$X_m(f) = \int dt \, \exp(-i2\pi ft) \, w_m(t) \, x(t) \quad \text{for } 1 \leq m \leq N,$$

$$Y_n(f) = \int dt \, \exp(-i2\pi ft) \, w_n(t) \, y(t) \quad \text{for } 1 \leq n \leq N. \tag{1}$$

These temporal weightings are generally taken as delayed versions of a basic weighting $w(t)$ according to

$$w_n(t) = w(t-nS), \tag{2}$$

where S is a shift or time delay; however, we keep the more general case in (1) for the time being.

The cross-spectral density estimate at frequency f is obtained by multiplying outputs (1) and averaging in time according to

$$v \equiv \sum_{n=1}^{N} X_n(f) \, Y_n^*(f). \tag{3}$$

This is the product array output; it has resolution capability in the spatial angles by virtue of each array output being steered to the same desired look direction, and it has frequency resolution governed by the lengths of the weightings in (1) or (2).

The mean of a general product term of components of (1) is

---

*An integral without limits is over the entire range of its non-zero integrand.

$$\overline{X_m(f)Y_n^*(f)} = \iint dt\ du\ \exp[-i2\pi f(t-u)]\ w_m(t)\ w_n(u)\ R_{xy}(t-u) =$$
$$= \int d\tau\ \exp(-i2\pi f\tau)\ R_{xy}(\tau)\ \phi_{mn}(\tau) = G_{xy}(f) \circledast \Phi_{mn}(f) =$$
$$= \int du\ G_{xy}(u)\ \Phi_{mn}(f-u), \tag{4}$$

where

$$R_{xy}(\tau) = \overline{x(t)\ y(t-\tau)} \tag{5}$$

is the cross-correlation of array outputs,

$$\phi_{mn}(\tau) = \int dt\ w_m(t)\ w_n(t-\tau) \tag{6}$$

is the aperiodic correlation of w_m and w_n, $\circledast$ denotes convolution, and

$$\Phi_{mn}(f) = \int d\tau\ \exp(-i2\pi f\tau)\ \phi_{mn}(\tau) = W_m(f)\ W_n^*(f) \tag{7}$$

is the product of windows of the individual temporal weightings.

If cross-spectrum G_{xy} does not vary significantly in the width of window Φ_{mn}, (4) yields approximation

$$\overline{X_m(f)Y_n^*(f)} \cong G_{xy}(f) \int du\ \Phi_{mn}(f-u) = G_{xy}(f)\ \phi_{mn}(0). \tag{8}$$

Now we apply these results to find the mean of the system output cross-spectral density estimate in (3):

$$\mu_v = \bar{v} = G_{xy}(f) \sum_{n=1}^{N} \phi_{nn}(0) = G_{xy}(f) \sum_{n=1}^{N} \int dt\ w_n^2(t), \tag{9}$$

which is proportional to the true cross-spectral density G_{xy} between the two array outputs.

In order to evaluate the variance of system output v in (3), we need magnitude-square value (suppressing f)

$$\overline{|v|^2} = \sum_{m,n=1}^{N} \overline{X_m Y_m^* X_n^* Y_n}. \tag{10}$$

We assume that the filtered outputs X_m and Y_n in (1) are complex Gaussian (as, for example, if x(t) and y(t) were Gaussian). We then observe that

$$\overline{X_m Y_n} = \iint dt\, du\, \exp[-i2\pi f(t+u)]\, w_m(t)\, w_n(u)\, R_{xy}(t-u) =$$

$$= \int d\nu\, G_{xy}(\nu)\, W_m(f-\nu) W_n(f+\nu). \tag{11}$$

Now for f removed from zero by at least the reciprocal of the segment length, the two windows in (11) do not overlap, and we get

$$\overline{X_m\, Y_n} \cong 0 \text{ for } f \neq 0 . \tag{12}$$

Then using the factoring property of zero-mean Gaussian random variables, (10) becomes

$$\overline{|v|^2} = \sum_{m,n=1}^{N} \left[\overline{X_m Y_m^*}\, \overline{X_n^* Y_n} + \overline{X_m X_n^*}\, \overline{Y_m^* Y_n} \right], \tag{13}$$

where we used (12). The variance of random variable v is

$$\sigma_v^2 = \overline{|v-\overline{v}|^2} = \overline{|v|^2} - |\overline{v}|^2 = \sum_{m,n=1}^{N} \overline{X_m X_n^*}\, \overline{Y_m^* Y_n} =$$

$$= \sum_{m,n=1}^{N} [G_x(f) \circledast \Phi_{mn}(f)][G_y(f) \circledast \Phi_{mn}^*(f)] =$$

$$\cong G_x(f)\, G_y(f) \sum_{m,n=1}^{N} \phi_{mn}^2(0) , \tag{14}$$

where we used (9), (4), and (8).

We now specialize the general weightings in (1) to the particular case in (2), obtaining from (6)

$$\phi_{mn}(0) = \int dt\; w(t-mS)\; w(t-nS) = \phi_w((n-m)S), \tag{15}$$

where

$$\phi_w(\tau) = \int dt\; w(t)\; w(t-\tau) \tag{16}$$

is the aperiodic correlation of basic temporal weighting w. Then variance σ_v^2 in (14) becomes

$$\sigma_v^2 = G_x(f)\; G_y(f) \sum_{m,n=1}^{N} \phi_w^2((n-m)S) = G_x(f)\; G_y(f) \sum_{p=1-N}^{N-1} (N-|p|)\; \phi_w^2(pS)\ . \tag{17}$$

We are now in position to formulate a quality ratio for the output of the product array. Namely we define the complex (voltage) quality ratio

$$\frac{\mu_v}{\sigma_v} = \sqrt{N}\,\gamma_{xy}(f) \left[\sum_{p=1-N}^{N-1} \left(1 - \frac{|p|}{N}\right) \frac{\phi_w^2(pS)}{\phi_w^2(0)}\right]^{-1/2}, \tag{18}$$

where we define the complex coherence between the array outputs as

$$\gamma_{xy}(f) = \frac{G_{xy}(f)}{[G_x(f)\; G_y(f)]^{1/2}}, \tag{19}$$

and have employed (9), (17), and (15). The quantity in (18) is desired large; it has leading factor $\sqrt{N}$, which however is partially compensated by the last factor of (18) if shift S is less than the segment length of temporal weighting w. A detailed investigation of the temporal processing factors in (18) is given in [1]; for present purposes, the factor is nearly maximized if shift S is taken about 50% of the segment length.

However, the most important quantity in quality ratio (18) is the complex coherence at frequency f, $\gamma_{xy}(f)$. It is always bounded in magnitude by 1, and can be significantly less than 1 if the two array outputs x(t) and y(t) are incoherent at frequency f of interest.

On the other hand, for identical arrays and array weightings, we have $y(t) = x(t)$, and the quality ratio is again given by (18), where $\gamma_{xy}(f)$ is replaced by

$$\gamma_{xx}(f) = 1. \tag{20}$$

That is, the sum array and product array differ in their complex quality ratios simply by the factor $\gamma_{xy}(f)$, which is the complex coherence of the two arrays in the product formulation. Thus the relative performance of a product array can be investigated by determining the coherence of its component array outputs.

With this information, we can now give a qualitative measure of performance of the cross-line array. Consider two line arrays lying along the horizontal and vertical axes, respectively. Suppose both lines are steered to the same look direction in three-dimensional space. Since a line array must inherently have maximum response everywhere in a cone of symmetry centered on the line, the two cones will intersect at the desired look direction, but will have largely non-overlapping cones at other angles. Thus only a small fraction of the output of each array is in common; in fact, most of each array output comes from <u>uncommon</u> arrival angles.

Thus the two line array outputs will be largely independent of each other, meaning low coherence. Furthermore, the longer the line arrays, the finer becomes the angular resolution, and the common intersection volume of the cones decreases. Thus the performance of the product array relative to the sum array becomes poorer as the line arrays become longer. In the next section, these conclusions will be verified by a detailed quantitative analysis of the coherence between two general array outputs.

CROSS-SPECTRUM OF INDIVIDUAL ARRAY OUTPUTS

Let the pressure field at time t and general location x,y in a planar array be denoted by $p(t,x,y)$. Let the field be stationary and homogeneous, with temporal-spatial correlation

$$\overline{p(t_1,x_1,y_1)\ p(t_2,x_2,y_2)} = R_p(t_1-t_2,x_1-x_2,y_1-y_2) \ . \tag{21}$$

The frequency-wavenumber spectrum corresponding to R_p is $\Phi_p(f,\mu,\nu)$, where

$$R_p(\tau,u,v) = \iiint df\ d\mu\ d\nu\ \exp(i2\pi f\tau+iu\mu+iv\nu)\ \Phi_p(f,\mu,\nu) \ . \tag{22}$$

We also define a partial transform of (22) as

$$\mathcal{G}_p(f,u,v) = \iint d\mu\ d\nu\ \exp(iu\mu+iv\nu)\ \Phi_p(f,\mu,\nu) \ . \tag{23}$$

This mixed function of temporal frequency and spatial separations will be of prime importance later, especially if it can be evaluated in closed form.

The grid structure of the planar array is such that the elements are equi-spaced, being located at positions md,nd in the x,y plane, for m,n integer. If a particular element is absent or is not used in an array output, the weighting of that element output is simply set equal to zero. For polar angle ϕ as measured from the z-axis, and azimuthal angle θ as measured from the x-axis, the time delay τ_{mn} employed at location md,nd, in order to steer in desired look direction ϕ_ℓ, θ_ℓ, is [2, Appendix A]

$$\tau_{mn} = -\frac{d}{c}(\alpha m+\beta n) \ , \tag{24}$$

where d is the element spacing, c is the speed of propagation, and

$$\alpha = \sin\phi_\ell\ \cos\theta_\ell \ , \ \beta = \sin\phi_\ell\ \sin\theta_\ell \ . \tag{25}$$

Broadside to the planar array corresponds to $\phi_\ell = 0$.

Array output $x(t)$ is synthesized by choosing a particular subset of elements in the planar grid structure, weighting their outputs, and time-delay steering to the desired look direction ϕ_ℓ, θ_ℓ . Thus*

$$x(t) = \sum_{k\ell} w_x(k,\ell)\ p(t-\tau_{k\ell},\ kd,\ \ell d)\ . \tag{26}$$

By simply setting some weights to zero, a line array or a cross-line, or any desired array configuration, can be realized. Similarly, a second array output, which may employ some or all of the same elements, is

$$y(t) = \sum_{mn} w_y(m,n)\ p(t-\tau_{mn},\ md,\ nd)\ . \tag{27}$$

The cross-correlation of array outputs (26) and (27) is, upon use of (21),

$$R_{xy}(\tau) = \overline{x(t)y(t-\tau)} = \sum_{k\ell mn} w_x(k,\ell)\ w_y(m,n)\ R_p(\tau+\tau_{mn}-\tau_{k\ell},(k-m)d,(\ell-n)d). \tag{28}$$

Using (23) and (24), the cross-spectrum of x and y is

$$\begin{aligned} G_{xy}(f) &= \sum_{k\ell mn} w_x(k,\ell)\ w_y(m,n)\ \exp[i2\pi f(\tau_{mn}-\tau_{k\ell})]\ \mathcal{G}_p(f,(k-m)d,(\ell-n)d) = \\ &= \sum_{k\ell mn} w_x(k,\ell)\ w_y(m,n)\ \exp[i2\pi f\tfrac{d}{c}(\alpha k+\beta\ell-\alpha m-\beta n)]\ \mathcal{G}_p(f,(k-m)d,(\ell-n)d) = \\ &= \sum_{qr} \phi_{xy}(q,r)\ \exp\left[i2\pi f\tfrac{d}{c}(\alpha q+\beta r)\right] \mathcal{G}_p(f,qd,rd)\ , \end{aligned} \tag{29}$$

where we let q=k−m, r= −n, and defined

$$\phi_{xy}(q,r) = \sum_{k\ell} w_x(k,\ell)\ w_y(k-q,\ell-r) \tag{30}$$

*A summation without limits is over the entire range of its non-zero summand.

as the two-dimensional cross-correlation of the weight structure employed to yield array outputs x(t) and y(t).

As the first special case of the above, a pair of perpendicular cross-lines can be realized by setting

$$w_x(k,\ell) = 0 \text{ except for } \ell = 0,$$
$$w_y(m,n) = 0 \text{ except for } m = 0; \tag{31}$$

in this case, (30) yields

$$\phi_{xy}(q,r) = w_x(q,0)\ w_y(0,-r), \tag{32}$$

and (29) becomes the cross-spectrum of the cross-line array,

$$G_{xy}^{(c)}(f) = \sum_{qr} w_x(q,0)\ w_y(0,-r)\ \exp[i2\pi f\tfrac{d}{c}(\alpha q+\beta r)]\ \mathcal{G}_p(f,qd,rd). \tag{33}$$

A second special case is obtained by considering the sum array, which corresponds to setting

$$w_x(k,\ell) = w_y(k,\ell) = w(k,\ell), \tag{34}$$

thereby getting from (30)

$$\phi_{xy}(q,r) = \sum_{k\ell} w(k,\ell)\ w(k-q,\ell-r) \equiv \phi_s(q,r)\ , \tag{35}$$

and from (29), the auto-spectrum of the sum array,

$$G_{xy}^{(s)}(f) = \sum_{qr} \phi_s(q,r)\ \exp[i2\pi f\tfrac{d}{c}(\alpha q+\beta r)]\ \mathcal{G}_p(f,qd,rd)\ . \tag{36}$$

Comparison of special cases (33) and (36) reveals that the mean responses of the cross-line and sum arrays can be made equal by setting

$$w_x(q,0)\ w_y(0,-r) = \phi_s(q,r) = \sum_{k\ell} w(k,\ell)\ w(k-q,\ell-r) \text{ for all } q,\ r\ . \tag{37}$$

So, for example, if the sum weighting $w(k,\ell)$ is flat over a rectangle, $\phi_s(q,r)$ is triangular in q as well as r, over a rectangle twice the size. Thus, if line weightings $w_x(q,0)$ and $w_y(0,-r)$ are each triangular over this double-length, (37) is satisfied, and $G_{xy}^{(c)}(f) = G_{xy}^{(s)}(f)$. This conclusion holds irrespective of the pressure field statistics $\mathcal{R}_p(f,qd,rd)$.

Returning now to the general case of (29) and (30), the auto-spectrum $G_x(f)$ of array output x(t) in (26) is easily obtained by replacing w_y by w_x in (30) and using that result for ϕ_{xy} in (29). A similar procedure, but now replacing w_x by w_y, yields the auto-spectrum $G_y(f)$ of array output y(t) in (27). Combined with (29) itself, we now have the capability of calculating coherence $\gamma_{xy}(f)$ as given earlier by (19).

An alternative illuminating form for cross-spectrum $G_{xy}(f)$ is obtained by substituting, for $\mathcal{R}_p$ in the second line of (29), the expression (23) and interchanging summation and integration:

$$G_{xy}(f) = \iint d\mu\ d\nu\ \Phi_p(f,\mu,\nu) *$$

$$* W_x(2\pi f\tfrac{d}{c}\alpha+d\mu,\ 2\pi f\tfrac{d}{c}\beta+d\nu)\ W_y^*(2\pi f\tfrac{d}{c}\alpha+d\mu,\ 2\pi f\tfrac{d}{c}\beta+d\nu)\ , \tag{38}$$

where

$$W_x(a,b) = \sum_{k\ell} w_x(k,\ell)\ \exp(ika+i\ell b),$$

$$W_y(a,b) = \sum_{mn} w_y(m,n)\ \exp(ima+inb)\ , \tag{39}$$

are the response patterns of the x and y arrays. Since the patterns in (39) peak at a = b = 0, the integral in (38) is dominated by the contribution at spatial frequencies

$$\mu = -2\pi\frac{f}{c}\alpha = -\frac{2\pi}{\lambda}\sin\phi_\ell\cos\theta_\ell\ ,$$

$$\nu = -2\pi\frac{f}{c}\beta = -\frac{2\pi}{\lambda}\sin\phi_\ell\sin\theta_\ell\ . \tag{40}$$

That is, the cross-spectrum in (38) is influenced mainly by frequency-wavenumber spectrum value $\Phi_p(f,\mu,\nu)$ at the values given by (40). $\lambda=c/f$ is the wavelength at the frequency f of interest.

EXAMPLES OF FREQUENCY-WAVENUMBER SPECTRA

Square Support

Suppose that at some frequency $f=f_o$, the frequency-wavenumber spectrum is flat over a square:

$$\Phi_p(f_o,\mu,\nu) = \left\{ \begin{array}{l} \Phi_1(f_o)\,\dfrac{1}{4k_L^2} \quad \text{for } |\mu| < k_L,\ |\nu| < k_L \\ \\ \quad 0 \quad \text{otherwise} \end{array} \right\}, \tag{41}$$

where k_L is the common limit of wavenumbers in μ and ν. Then from (23),

$$\mathcal{B}_p(f_o,u,v) = \Phi_1(f_o)\,\frac{\sin(k_L u)}{k_L u}\,\frac{\sin(k_L v)}{k_L v}\,. \tag{42}$$

This closed-form expression is separable in u and v and will lead to worthwhile simplifications when employed in (29), and especially cross-line result (33).

Circular Support

Suppose instead that

$$\Phi_p(f_o,\mu,\nu) = \left\{ \begin{array}{l} \Phi_1(f_o)\,\dfrac{1}{\pi k_L^2} \quad \text{for } \mu^2 + \nu^2 < k_L^2 \\ \\ \quad 0 \quad \text{otherwise} \end{array} \right\}. \tag{43}$$

Then (23) yields

$$\mathcal{B}_p(f_o,u,v) = \Phi_1(f_o)\,\frac{2J_1\left(k_L\sqrt{u^2+v^2}\right)}{k_L\sqrt{u^2+v^2}}\,, \tag{44}$$

which has circular symmetry in separation space u,v. Although in closed form, it is not separable in u and v, and is more time-consuming to evaluate than (42).

CROSS-LINE ARRAY WITH SQUARE-SUPPORT SPECTRUM

In this section, we specialize to a cross-line array as depicted in figure 1 and couple it with the square-support frequency-wavenumber spectrum

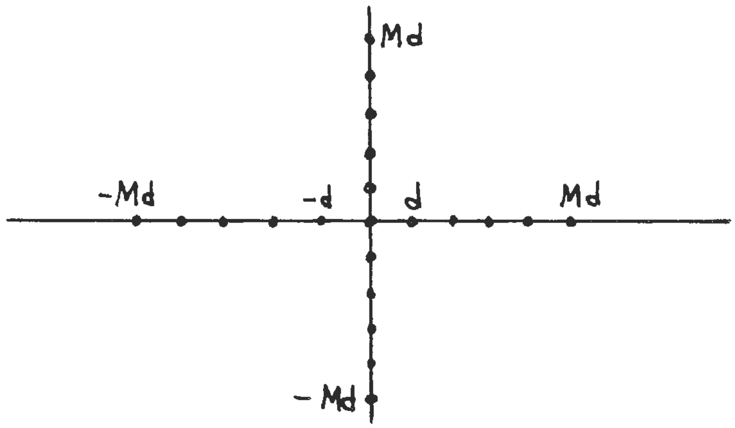

Figure 1. Cross-Line Array of 4M+1 Elements

of (41). The cross-line array has one element at the origin and M elements in each of the four perpendicular legs protruding from the origin, for a total of 4M+1 elements. All elements are spaced by d in both directions, consistent with (24)-(27).

The cross-spectrum at frequency f_o, between the two perpendicular lines, is given by (33) with (42):

$$G_{xy}^{(c)}(f_o) = \Phi_1(f_o) \sum_{qr} w_x(q,0)\, w_y(0,-r)\, \exp[ik_o d(\alpha q+\beta r)]\, \frac{\sin(k_L dq)}{k_L dq}\, \frac{\sin(k_L dr)}{k_L dr} =$$

$$= 4\Phi_1(f_o) \sum_{q=0}^{M} \varepsilon_q w_x(q,0)\cos(k_o d\alpha q)\, \frac{\sin(k_L dq)}{k_L dq} \sum_{r=0}^{M} \varepsilon_r w_y(0,r)\cos(k_o d\beta r)\, \frac{\sin(k_L dr)}{k_L dr}, \quad (45)$$

where

$$k_o \equiv \frac{2\pi}{\lambda_o} = 2\pi f_o/c\ , \qquad \varepsilon_q \equiv \left\{\begin{matrix} 1/2 & \text{for} & q = 0 \\ 1 & \text{for} & q \geq 1 \end{matrix}\right\}, \quad (46)$$

and the weight structure on each line has been assumed real and symmetric about the origin. The quantities in (45) are all real and require only two single-summations of size M at each value of the three dimensionless parameters $k_o d\alpha$, $k_o d\beta$, $k_L d$. Here, k_L is the common limit on allowed wavenumbers in square-support spectrum (41), and k_o is the wavenumber corresponding to frequency f_o of interest. Quantities α and β are given in terms of the look direction according to (25).

To find the auto-spectrum of line-array output x(t), we replace w_y by w_x in (30) and use the upper line of (31):

$$\phi_{xx}(q,r) = \sum_k w_x(k,0)\, w_x(k-q,-r) = \Psi_{xx}(q)\, \delta_{ro}, \tag{47}$$

where

$$\Psi_{xx}(q) \equiv \sum_k w_x(k,0)\, w_x(k-q,0) \tag{48}$$

is the auto-correlation of the x-array weights. Substitution of (47) in (29) yields

$$G_x^{(c)}(f_o) = \sum_q \Psi_{xx}(q) \exp(ik_o d\alpha q)\, \mathcal{G}_p(f_o,qd,0) =$$

$$= 2\, \Phi_1(f_o) \sum_{q=0}^{2M} \epsilon_q\, \Psi_{xx}(q) \cos(k_o d\alpha q)\, \frac{\sin(k_L dq)}{k_L dq}, \tag{49}$$

where we used (42) and (46). In a similar fashion, the auto-spectrum of line-array output y(t) is given by

$$G_y^{(c)}(f_o) = 2\Phi_1(f_o) \sum_{r=0}^{2M} \epsilon_r\, \Psi_{yy}(r) \cos(k_o d\beta r)\, \frac{\sin(k_L dr)}{k_L dr}\ , \tag{50}$$

where

$$\Psi_{yy}(r) \equiv \sum_{\ell} w_y(0,\ell)\; w_y(0,\ell - r)\;, \tag{51}$$

in keeping with (31). The auto-spectral results in (49) and (50) each require real single-sums of size 2M. No double summations are required in the cross-spectral result of (45) or in the auto-spectral results of (49) and (50), although in the latter cases, the auto-correlations Ψ_{xx} and Ψ_{yy} must be pre-computed. The complex coherence at frequency f_o, $\gamma_{xy}^{(c)}(f_o)$, between individual array outputs x(t) and y(t) of the cross-line, is given by ratio (19) as usual; the factor $\Phi_1(f_o)$, as well as the absolute scales of the weight structures $\{w_x(k,0)\}$, $\{w_y(0,\ell)\}$, will cancel out in the ratio. The fundamental parameters are $k_o d\alpha$, $k_o d\beta$, $k_L d$.

For broadside steering of the cross-line array, we have $\phi_\ell = 0$ and (25) yields $\alpha = \beta = 0$. Then (45), (49), (50) are independent of k_o, and the coherence depends only on $k_L d$.

CROSS-LINE ARRAY WITH CIRCULAR-SUPPORT SPECTRUM

By combining (33) with the circular-support frequency-wavenumber spectrum of (44), and using assumed symmetry of the line-array weights, we obtain cross spectrum

$$G_{xy}^{(c)}(f_o) = 4\Phi_1(f_o) \sum_{q=0}^{M} \varepsilon_q w_x(q,0)\cos(k_o d\alpha q) \sum_{r=0}^{M} \varepsilon_r w_y(0,r)\cos(k_o d\beta r)\frac{2J_1(k_L d\sqrt{q^2+r^2})}{k_L d\sqrt{q^2+r^2}}. \qquad (52)$$

This double sum can no longer be separated into the product of two single sums, as (45) was, due to the coupling caused by the Bessel function. However, the Bessel function need only be computed in a 45° sector of the q,r plane and then reflected about the 45° line; i.e., the same value is attained for q,r = m,n as for q,r = n,m.

The auto-spectrum of the x-array output is obtained by utilizing (44) in the top line of (49):

$$G_x^{(c)}(f_o) = 2\Phi_1(f_o) \sum_{q=0}^{2M} \varepsilon_q \Psi_{xx}(q) \cos(k_o d\alpha q) \frac{2J_1(k_L dq)}{k_L dq}, \qquad (53)$$

where Ψ_{xx} is again given by (48). In a similiar fashion, there follows

$$G_y^{(c)}(f_o) = 2\Phi_1(f_o) \sum_{r=0}^{2M} \varepsilon_r \Psi_{yy}(r) \cos(k_o d\beta r) \frac{2J_1(k_L dr)}{k_L dr}. \qquad (54)$$

The coherence is now available from (52)-(54). This example was not pursued numerically.

RESULTS

A program for the calculation of the coherence of a cross-line array, via (45)-(51), is given in appendix A. It was exercised to give the following results in figures 2-6. Although these plots look virtually identical, closer inspection of the numerical values (not included) reveals that there are small (insignificant) differences, even for the widely different values of k_0d, ϕ_ℓ, θ_ℓ considered here. The degradation of the cross-line array relative to the sum array is virtually independent of the particular look angle ϕ_ℓ, θ_ℓ. This can be partially explained by virtue of the fact that at broadside steering, a line array has a narrow beam but covers a full 360° angular sweep, whereas at endfire, the beam is broad but exists at only one angle. Thus the total angular coverage is essentially constant.

The overriding impression of figures 2-6 is that the degradation of the cross-line array is significant, relative to a sum array, in terms of the stability of the cross-spectral estimate. This is particularly so as the size of the array (4M+1 total elements) grows, or as k_Ld increases above .5. Further examples of interest may be obtained from the program in appendix A.

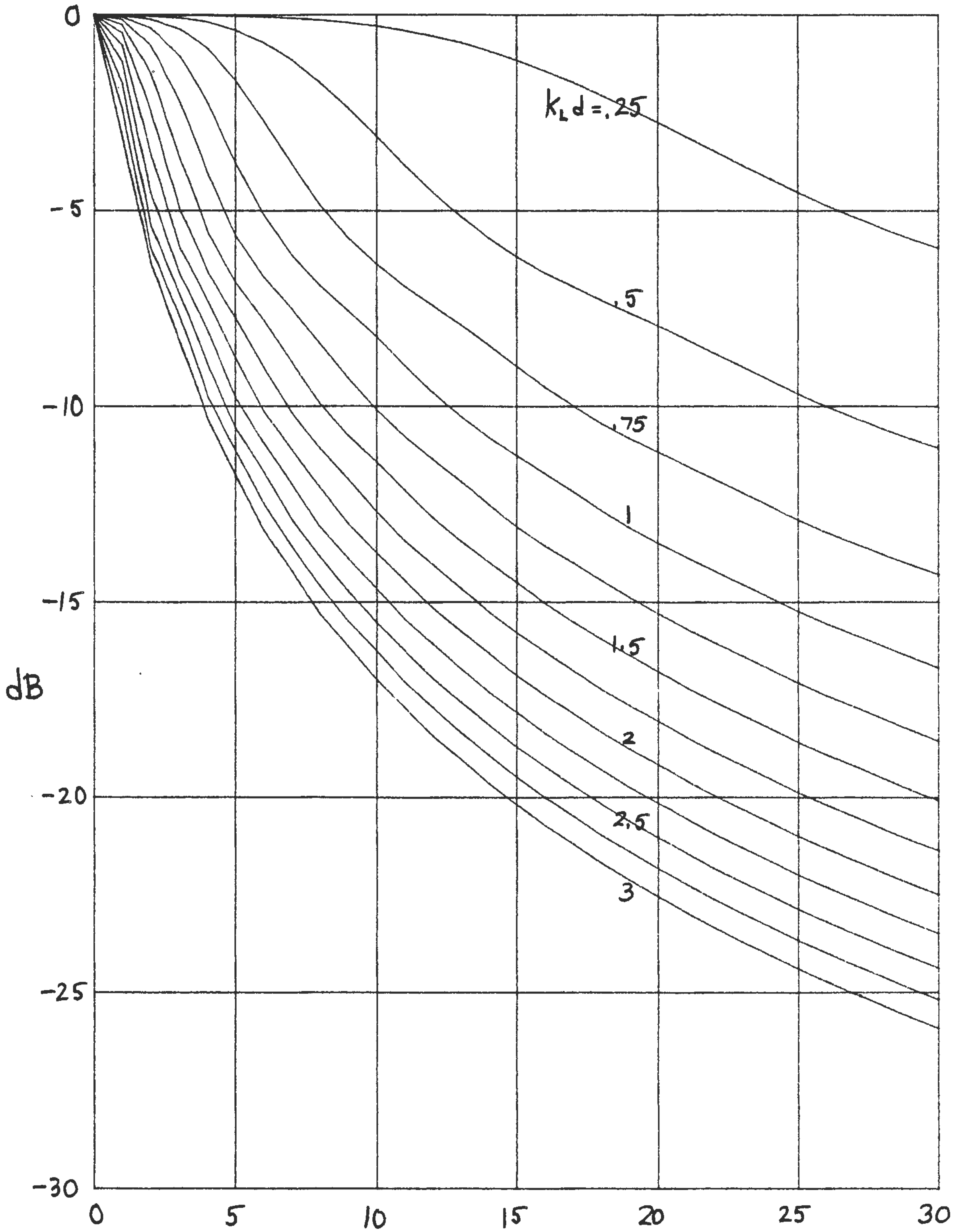

M, Number of Elements per Leg

Figure 2. Degradation for $k_0 d = \frac{\pi}{60}$, $\phi_\ell = 0$, $\theta_\ell = 0$

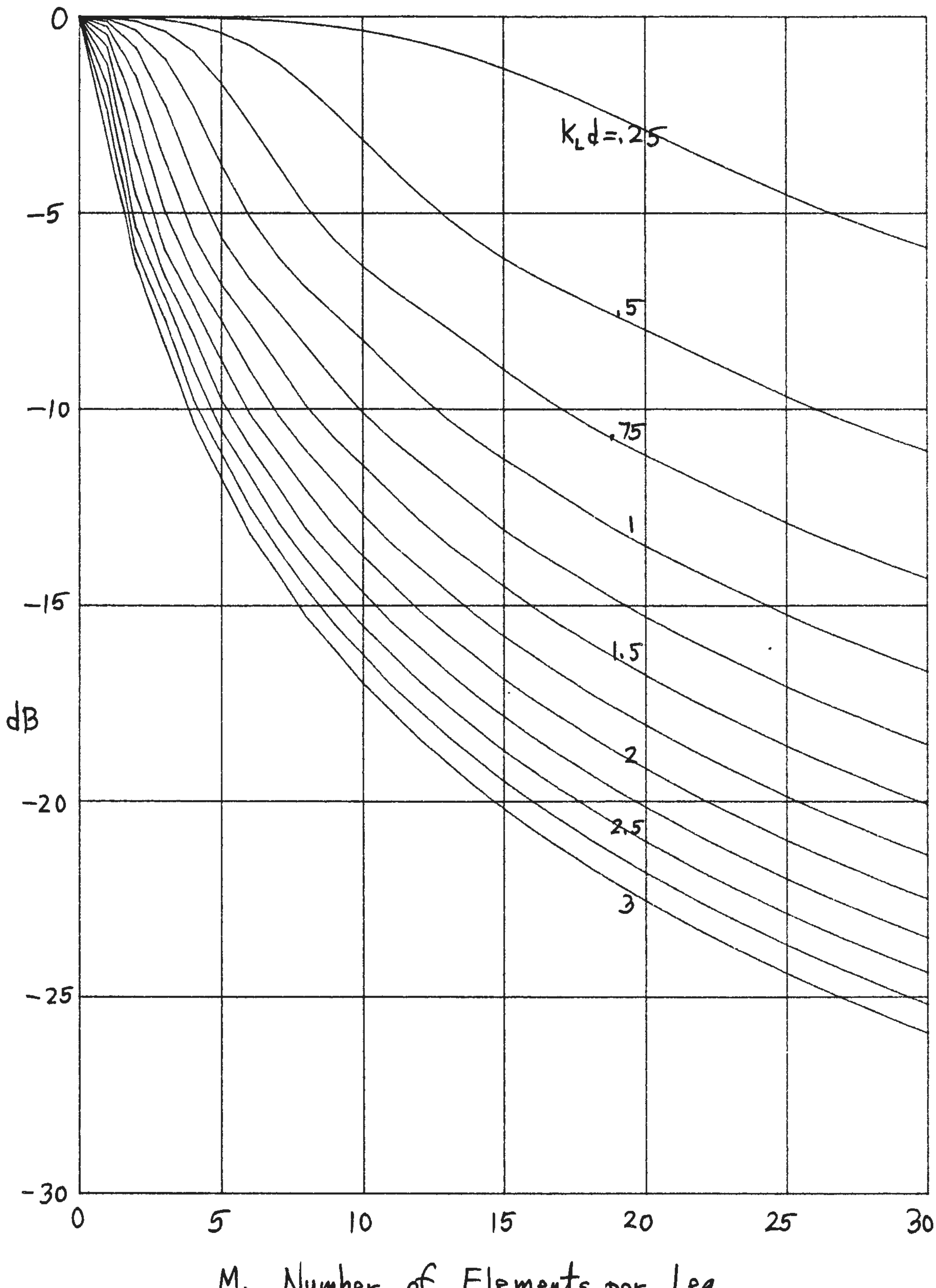

Figure 3. Degradation for $k_o d = \frac{\pi}{60}$, $\phi_\ell = \frac{\pi}{2}$, $\theta_\ell = 0$

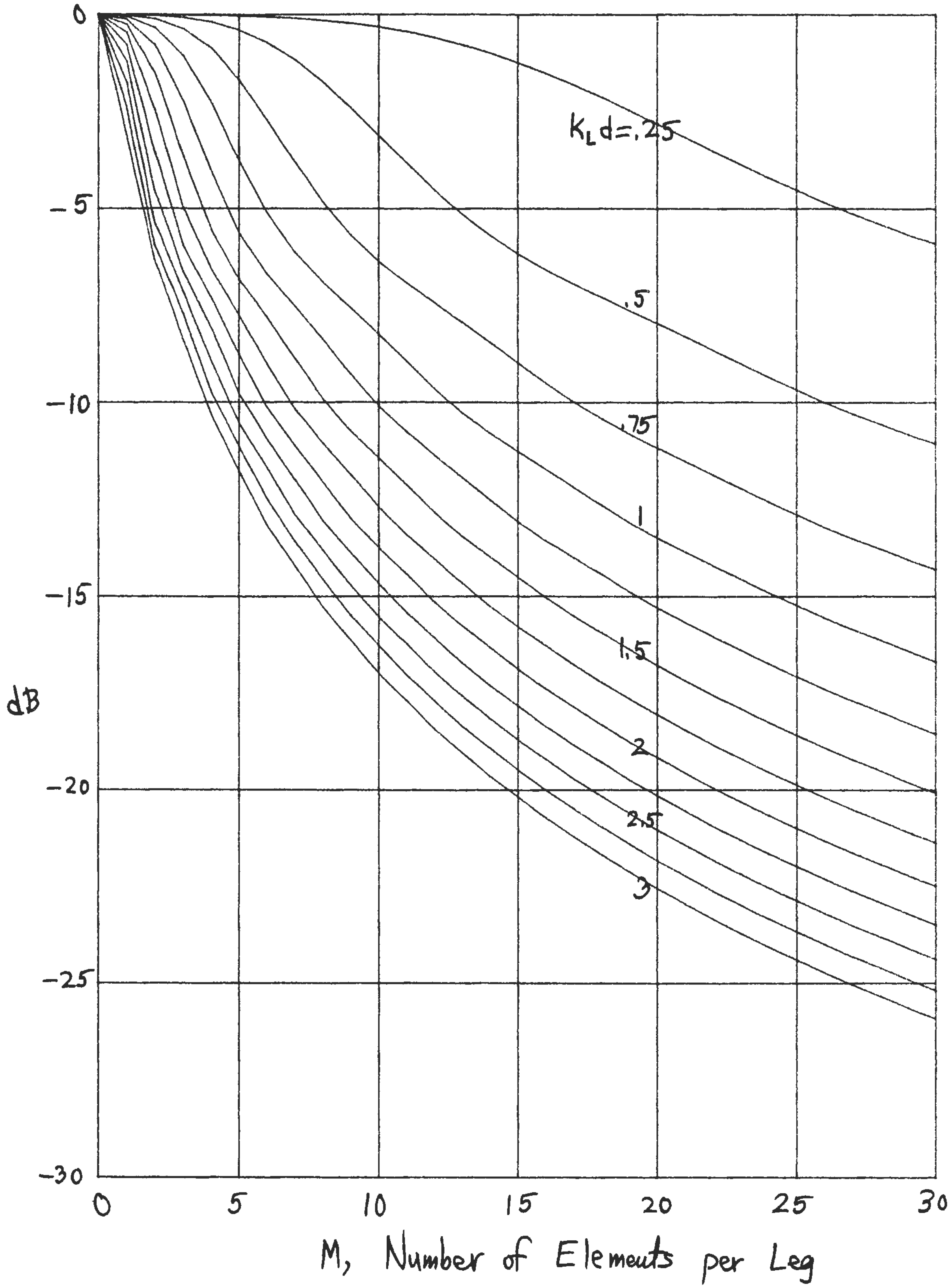

Figure 4. Degradation for $K_0 d = \frac{\pi}{60}$, $\phi_\ell = \frac{\pi}{4}$, $\theta_\ell = \frac{\pi}{4}$

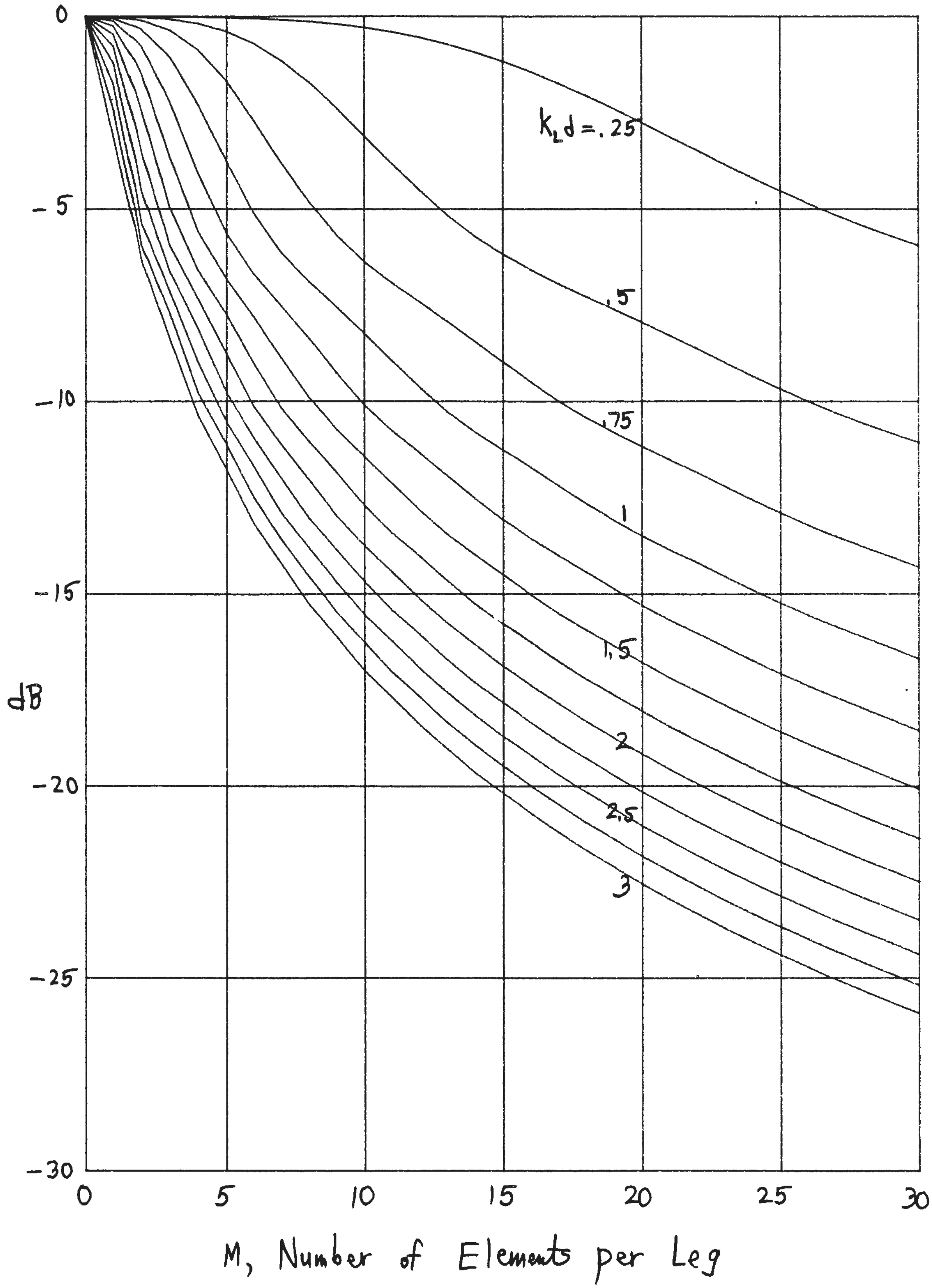

Figure 5. Degradation for $K_0 d = \frac{\pi}{150}$, $\phi_\ell = \frac{\pi}{4}$, $\theta_\ell = \frac{\pi}{4}$

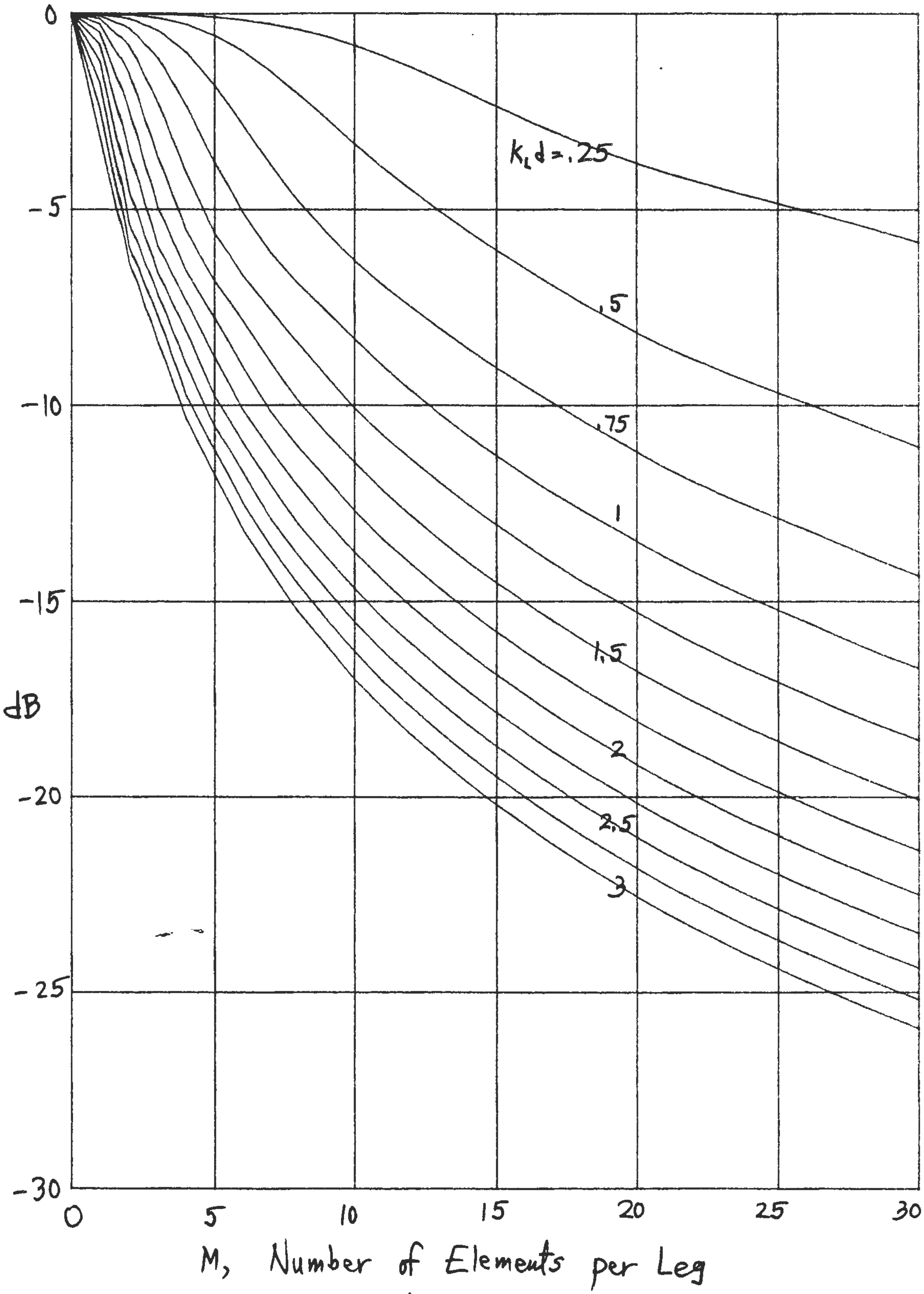

Figure 6. Degradation for $K_0 d = \frac{\pi}{15}$, $\phi_\ell = \frac{\pi}{4}$, $\theta_\ell = \frac{\pi}{4}$

SUMMARY

When the horizontal line array in figure 1 is time-delay steered to look in some desired direction ϕ_ℓ, θ_ℓ, it must also respond in a cone of symmetry centered on the axis of the line. Similarily, although the vertical line is steered to look in the same direction ϕ_ℓ, θ_ℓ, it too has a cone of equal response, but now centered on the vertical axis. These two cones will intersect at ϕ_ℓ, θ_ℓ and thereby lead to some common power at frequency f at their respective array outputs, prior to multiplication and averaging according to (3). However, both arrays also respond to uncommon (i.e. uncorrelated) power contributions from other directions, each within its own cone of response. The sharper the beams of each line array, the less common power will be intercepted, leading to less coherence between the two line outputs. Thus the stability of the cross-line array, relative to the sum array, degrades as the size of each line array increases.

If each of the product arrays were made of a parallel pair of lines (separated by some integer multiple of d), the responses of each would be rather complicated. However, there would again be some common overlap at ϕ_ℓ, θ_ℓ, but a great deal of uncommon response at other sidelobe regions, still causing a decreased coherence and unstable estimates. As more parallel lines are added to each product array, the performance should monotonically approach that of the sum array, being actually realized when all of the available parallel lines are employed, since the outputs of the horizontal and vertical arrays are then identical.

APPENDIX A. PROGRAM FOR CROSS-LINE ARRAY

The following program calculates the coherence of a cross-line array by means of (45)-(51). M is the number of elements in each of the four perpendicular legs protruding from the origin. The weighting in line 60 is assumed the same for both lines and is triangular. The autocorrelation of the weight structure is computed and stored in line 130. Inputs of $k_0 d$, ϕ_ℓ, θ_ℓ are required in lines 160-180 respectively. When these latter inputs are desired changed, the program can be continued at line 160 instead of 10, provided that the array weights have not also been changed. The input of $k_L d$ occurs in line 320. The dB output in line 520 is according to

$$dB = 10 \log_{10} \left|\gamma_{xy}(f_o)\right|^2 ,$$

since γ_{xy} is proportional to the voltage quality ratio.

```
10   DIM W(0:30,-30:30),Psi(0:30,0:60)
20   DIM Cosa(0:60),Cosb(0:60),Sinc(0:60),Db(0:30)
30   FOR M=0 TO 30
40   M1=M+1
50   FOR Ms=0 TO M
60   W(M,Ms)=W(M,-Ms)=1-Ms/M1          ! array weighting   triangular
70   NEXT Ms
80   FOR Qs=0 TO M+M
90   S=0
100  FOR Ms=Qs-M TO M
110  S=S+W(M,Ms)*W(M,Ms-Qs)
120  NEXT Ms
130  Psi(M,Qs)=S              !  auto-correlation of array weighting
140  NEXT Qs
150  NEXT M
```

```
160  Kod=PI/15                    !   INPUT
170  Polar=PI/4                   !   INPUT
180  Azimuth=PI/4                 !   INPUT
190  S=Kod*SIN(Polar)
200  Ta=S*COS(Azimuth)
210  Tb=S*SIN(Azimuth)
220  FOR Qs=0 TO 60
230  Cosa(Qs)=COS(Ta*Qs)
240  Cosb(Qs)=COS(Tb*Qs)
250  NEXT Qs
260  PLOTTER IS "9872A"
270  LIMIT 30,170,40,235
280  OUTPUT 705;"VS2"
290  SCALE 0,30,-30,0
300  GRID 5,5
310  PENUP
320  FOR K1d=.25 TO 3 STEP .25
330  Sinc(0)=1
340  FOR Qs=1 TO 60
350  S=K1d*Qs
360  Sinc(Qs)=SIN(S)/S
370  NEXT Qs
380  FOR M=0 TO 30
390  S1a=S1b=.5*W(M,0)
400  FOR Qs=1 TO M
410  S=W(M,Qs)*Sinc(Qs)
420  S1a=S1a+S*Cosa(Qs)
430  S1b=S1b+S*Cosb(Qs)
440  NEXT Qs
450  S2a=S2b=.5*Psi(M,0)
460  FOR Qs=1 TO M+M
470  S=Psi(M,Qs)*Sinc(Qs)
480  S2a=S2a+S*Cosa(Qs)
490  S2b=S2b+S*Cosb(Qs)
500  NEXT Qs
510  Coherence=2*S1a*S1b/SQR(S2a*S2b)
520  Db(M)=10*LGT(Coherence^2)
530  NEXT M
540  FOR M=0 TO 30
550  PLOT M,Db(M)
560  NEXT M
570  PENUP
580  NEXT K1d
590  END
```

REFERENCES

1. Nuttall, A. H., "Spectral Estimation by Means of Overlapped FFT Processing of Windowed Data", NUSC Report No. 4169, 13 October 1971.

2. Nuttall, A. H., "A Two-Parameter Class of Bessel Weightings with Controllable Sidelobe Behavior for Linear, Planar-Circular, and Volumetric-Spherical Arrays; The Ideal Weighting-Pattern Pairs", NUSC Technical Report 6761, 1 July 1982.

MEAN AND VARIANCE OF PRODUCT ARRAY RESPONSE:
APPLICATION TO A CROSS-LINE ARRAY

Albert H. Nuttall
Surface Ship Sonar Department
TM No. 841013
16 January 1984
UNCLASSIFIED

DISTRIBUTION LIST

EXTERNAL: CNM MAT 05B (CAPT. Z. L. NEWCOMB)
ONR 280 (J. Webster)
ONR 280 (D. Hurdis)
ONR 280 (R. Cantrell)
NSRDC, Code 19 (R. Stefanowicz)
BBN, Boston, MA (N. Martin)
BBN, Boston, MA (D. Korff)

B BUEHLER	3292	A LOTRING	02111
P CABLE	01Y	A NUTTALL	33
C CARTER	3314	N OWSLEY	3211
E EBY	101	A QUAZI	3314
A ELLINTHORPE	3292	C SHERMAN	3292
R ELSWICK	3233	W STRAWDERMAN	323
L FREEMAN	33	W VON WINKLE	10
J IANNIELLO	3212	LIBRARY GROUP, NLON 021311 (6 copies)	
R KNEIPFER	3212	LIBRARY GROUP, NWPT 021312 (3 copies)	

External: 7
Internal: 25
Total: 32